J Math Chem (2015) 53:250–259
DOI 10.1007/s10910-014-0425-y

ORIGINAL PAPER

Validation of convolution approximation to the thermal-average electron density

J. Robert Michael · Tibor Koritsanszky

Received: 26 August 2014 / Accepted: 30 September 2014 / Published online: 11 October 2014

Abstract Analytic evaluation of the dynamic (thermally smeared) molecular electron density (ED) is described within the LCAO-MO and harmonic-convolution approximations. The key step is to assign vibration probability density functions (PDFs) to the two-center products of Gaussian basis functions used in quantum chemical models, if the PDFs of the nuclear centers are known. Based on internal modes of vibrations of small molecules it is demonstrated how the convoluted ED relates to the stationary (static) ED, as well as to that of the average over an ensemble of static EDs calculated for near-equilibrium nuclear geometries using clamped Hamiltonians. The overall effect of neglecting correlated nuclear motions on the convoluted ED is also illuminated.

Keywords Electron density · Convolution · Mean square displacement amplitudes · Anisotropic displacement parameters · Linear combination of atomic orbitals molecular orbital · Bond critical point properties

Mathematics Subject Classification 26B40

1 Introduction

Analysis of high-resolution single-crystal X-ray diffraction data has become a routine procedure to elucidate the ED of solids [1,2]. This experimental route is considered by many investigators to be complementary or even alternative to the theoretical one offered by computational quantum chemistry, despite the vague link between the models as well as the driving principles utilized in the two methods. Nevertheless, for the

J. R. Michael · T. Koritsanszky (✉)
Center for Computational Sciences, Middle Tennessee State University, 1301 E. Main St., Murfreesboro, TN 37130, USA
e-mail: tkoritsa@mtsu.edu

lion's share of experimental reports the focus has chiefly been on validation of the results accomplished by comparing theoretical and experimental EDs, commonly in terms of Bond critical point (BCP) properties [3]. This collation is conceivable in two substantially different ways. In the usual course of modern X-ray studies an analytic Structure factor (SF) model (dominantly the rigid pseudoatom model [4,5]) is called upon that explicitly accounts for thermal smearing (density deformation due to nuclear vibrations) and whose static and dynamic parameters are jointly adjusted to the observed data using the standard Least-squares (LS) protocol. Such a fitting procedure allows for a technically straightforward and apparently satisfactory, yet intractable decoupling of thermal smearing effects from bonding effects [6,7]. In other words, the 'experimental' static ED and the Anisotropic displacement parameters (ADPs) obtained through such an analysis is unavoidably biased due to the failure of the applied scattering formalism to explicitly and adequately account for the physics underlying the coupling between electronic and nuclear motion.

A far less common method nowadays, but critically reflected on by the pioneers of the field [8,9], is to evaluate the vibration average of the theoretical ED using experimental ADPs. These efforts have been hampered by a number of issues/uncertainties; (a) the experimental ADPs have a limited physical significance, not only for the above mentioned reason, but also because these parameters are likely to absorb systematic errors and are affected by disorders (static and dynamic structural fluctuations); (b) internuclear correlations (vibration couplings) are not accessible from Bragg diffraction; (c) the lack of rigorous treatment of the vibration smearing of internuclear (two-center) density units. The latest issue, the subject of this paper, has been an indisputable source of bias in density matrix fitting [10–12] and wave function supported refinements (two-center ED models) of X-ray data [13].

It is to be emphasized that both approaches (that is, decoupling the thermal motion from the experimental ED or smearing the theoretical ED) rely on the harmonic-convolution approximation which is at the heart of modeling coherent elastic diffraction [14], but fails to comply with the Born–Oppenheimer approximation [15], which, on the other hand, is at the heart of molecular quantum chemistry. This contradiction provokes the plain questions; are the theoretical and 'experimental' EDs comparable at all and what can we reasonably expect to learn from their agreement/disagreement after all?

Assessment of the convolution approximation has been the subject matter of computational studies on small molecules [16,17] as well as temperature dependent diffraction analyses [18,19]. The temperature independence of experimental static BCP properties has often been used to infer the 'thermal-decoupling capability' of a scattering/static ED model used for the analysis of the diffraction data [20].

In this study we evaluate the theoretical dynamic molecular ED derived as the exact convolution of the nuclear PDF for harmonic internal vibrations with the static molecular ED given within the Linear combination of atomic orbitals molecular orbital (LCAO-MO) formalism in terms of Gaussian basis functions. The convoluted dynamic ED is compared with the mean ED obtained within the adiabatic approximation [21] as the average over a large number of static EDs corresponding to nuclear configurations consistent with harmonic vibrations. Both the electronic and nuclear distributions are

derived according to standard computational chemistry protocols with the aid of the Gaussian09 program suite [22] and locally developed computer codes [23].

2 The convolution approximation

The key property for interpreting X-ray Bragg scattering is the coherent elastic SF, the Fourier transform of the thermal average (T-dependent canonical ensemble average over vibration states) of the crystalline ED (referred here as the dynamic ED):

$$\langle \rho \rangle_T = \sum_n w_n \rho_n \tag{1}$$

where w_n and ρ_n is the Boltzmann factor and ED, respectively, associated with the nth state of the system in thermal equilibrium with its surrounding. To reduce this expression to a closed analytic form applicable to SF data fitting, the harmonic convolution approximation is invoked which includes a hierarchy of approximations [24]: (a) the states accessible by the system (molecule or crystal) are restricted to vibration states (no electronic transition occurs during scattering); (b) the adiabatic approximation that implicitly assumes the physical observability of the stationary ED corresponding to the equilibrium nuclear geometry (represented hereafter by a $3N$-row-vector $\boldsymbol{R}^0$ for N nuclei); (c) the stationary ED is supposed to be expressed as a superposition of partial distributions each assigned to a specific center; (d) even less feasibly, each such density unit is defined to rigidly follow the motion of its center as the nuclei vibrate about their equilibrium positions in a harmonic potential.

The normal mode analysis of the system of N vibrating nuclei in thermal equilibrium leads to a $3N$-multivariate normal distribution of nuclear displacements relative to their equilibrium positions ($\boldsymbol{u} = \boldsymbol{R} - \boldsymbol{R}^0$):

$$P(\boldsymbol{u}) = (2\pi)^{\frac{-3N}{2}} |\boldsymbol{U}|^{-\frac{1}{2}} Exp\left[-\frac{1}{2}\boldsymbol{u}\boldsymbol{U}^{-1}\bar{\boldsymbol{u}}\right] \tag{2}$$

where $\bar{\boldsymbol{u}}$ denotes the transpose of $\boldsymbol{u}$ and the covariance matrix is the Mean square displacement amplitude (MSDA) matrix ($\boldsymbol{U}$) associated with the expectation values of Cartesian nuclear displacement products (second moments):

$$\boldsymbol{U} = \langle \bar{\boldsymbol{u}}\boldsymbol{u} \rangle_T \tag{3}$$

The temperature dependence of $\boldsymbol{U}$ is embedded in the MSDAs of the normal modes, since for the eigenvalues ($\boldsymbol{\delta} = (\delta_{i=1,3N})$):

$$\boldsymbol{U} = \boldsymbol{L}\boldsymbol{\delta}\bar{\boldsymbol{L}} \tag{4}$$

$$\delta_j = \frac{h}{8\pi^2 \nu_j} \coth\left(\frac{h\nu_j}{2k_B T}\right) \tag{5}$$

where ν_j is the frequency of the jth normal mode [25,26].

In the simplest versions of the Bragg SF formalism, that relies on the one-center ED models (such as the conventional isolated-atom or the pseudoatom; nucleus-centered multipole expansion [4,5]), the correlations between nuclear vibrations are ignored. In other words, the density units centered on a given nucleus ($\rho_a(\boldsymbol{r}_a), \boldsymbol{r}_a = \boldsymbol{r} - \boldsymbol{R}_a$) are smeared (convoluted) by a trivariate normal distribution of that nuclear center (marginal PDF; P_a). This means that the $3N$ multivariable normal distribution is taken as a product of N trivariate normal distributions, giving rise to the smeared ED

$$\langle \rho(\boldsymbol{r}) \rangle_T = \sum_a \int_{-\infty}^{\infty} \rho_a(\boldsymbol{r_a} - \boldsymbol{u}) P_a(\boldsymbol{u}) \, d\boldsymbol{u} \tag{6}$$

Note that the Fourier transform of a marginal PDF (P_a) is the Debye–Waller (DW) factor routinely used in scattering models to dampen the scattering power of an atom due to nuclear vibrations [27,28].

If the convolution approximation is to be applied to the ED within the LCAO-MO approach, new considerations arise because it is not immediately apparent how to calculate the ADPs of non-nuclear sites at which two-center orbital products are centered. Approximations of practical relevance have been suggested previously to estimate the variance/DW factor of these centers as a linear combination of experimental nuclear ADPs [29]/DW factors [10,30,31], but without providing the exact solution given below.

3 Convolution of two-center Gaussian basis products

Within the LCAO-MO approach, the ED can be expressed as a linear combination of basis function products:

$$\rho(\boldsymbol{r}) = \sum_{i,j}^{Nprims} C_{ij} \chi_i(\boldsymbol{r}) \chi_j(\boldsymbol{r}) \tag{7}$$

$$\chi_i(\boldsymbol{r}) = (x - X_i)^{n_i} (y - Y_i)^{m_i} (z - Z_i)^{l_i} Exp\left[-\alpha_i |\boldsymbol{r} - \boldsymbol{R}_i|^2\right] \tag{8}$$

where $\chi_i(\boldsymbol{r})$ is a (non-normalized) primitive Gaussian Type Orbital (GTO) centered at $\boldsymbol{R}_i = (X_i, Y_i, Z_i)$. The product of two primitive GTOs centered at (X_a, Y_a, Z_a) and (X_b, Y_b, Z_b) is also a GTO centered between the two [32].

Let $\boldsymbol{a} = (a_x, a_y, a_z) = (x - X_a, y - Y_a, z - Z_a)$ have a normal trivariate PDF with zero mean ($\langle \boldsymbol{a} \rangle = (0, 0, 0)$) and covariance $\boldsymbol{U}_{aa} = \{Cov(a_i, a_j) = \langle \bar{\boldsymbol{a}}\boldsymbol{a} \rangle\}$ (where i, j range over x, y, z), a 3×3 symmetric tensor, the ADPs of nucleus $\boldsymbol{R}_a$. If $\boldsymbol{b}$ is likewise defined with $\boldsymbol{U}_{bb}$, then the displacement vector of the GTO at $\boldsymbol{c}$ defined by the product of GTOs at $\boldsymbol{a}$ and $\boldsymbol{b}$ is

$$\boldsymbol{c} = \frac{\alpha \boldsymbol{a} + \beta \boldsymbol{b}}{\alpha + \beta} \tag{9}$$

where α and β are the exponents of the respective primitive GTOs of the product. The covariance matrix of center $\boldsymbol{c}$ is

$$\begin{aligned}\boldsymbol{U}_{cc} = \langle \bar{\boldsymbol{c}}\boldsymbol{c}\rangle &= \frac{\alpha^2\langle \bar{\boldsymbol{a}}\boldsymbol{a}\rangle + \alpha\beta\left(\langle \bar{\boldsymbol{a}}\boldsymbol{b}\rangle + \langle \bar{\boldsymbol{b}}\boldsymbol{a}\rangle\right) + \beta^2\langle \bar{\boldsymbol{b}}\boldsymbol{b}\rangle}{(\alpha+\beta)^2} \\ &= \frac{\alpha^2\boldsymbol{U}_{aa} + \alpha\beta\left(\boldsymbol{U}_{ab} + \boldsymbol{U}_{ba}\right) + \beta^2\boldsymbol{U}_{bb}}{(\alpha+\beta)^2}\end{aligned} \tag{10}$$

where $\boldsymbol{U}_{ba} = \bar{\boldsymbol{U}}_{ab}$ are the off-diagonal blocks of $\boldsymbol{U}$ representing the correlation between the vibration of nuclei $\boldsymbol{a}$ and $\boldsymbol{b}$. Eqn. 10 provides an exact representation for the ADPs of a product of primitive GTOs. To reproduce a situation in which the off diagonal blocks may be unknown, it is sufficient to set both $\boldsymbol{U}_{ab}$ and $\boldsymbol{U}_{ba}$ to zero. The methods described in this section are implemented in the current version of the Denprop [23] software package.

4 Results and discussion

The convolution formalism detailed above is applied to the LCAO-MO EDs of the formamide and the octasulfur molecules at the B3LYP/6-311G** [33] and MP2/cc-PVTZ [34] levels of theory, respectively, calculated at the equilibrium geometries using the Gaussian09 program suite [22]. The MSDAs corresponding to a temperature of 23 K were derived from the harmonic vibration frequencies and normal modes at the same levels of theory. The optimized geometries were obtained using the 'very tight' convergence criteria leading to small frequencies for the external modes. For the sake of simplicity, we imposed planarity for formamide, as this structure has been the subject of a vibration-smearing study [35] based on Fourier expansion and external ADPs. The lowest frequency (highest amplitude) mode is the NH_2 wagging ($\omega(NH_2)$) that displaces all three atoms out of the molecular (XY) plane. Since we consider only internal modes of vibration, the MSDA matrix has a rank of 3N-6. Nevertheless, the block diagonal matrices (the ADPs) are positive definite (with condition number >8) thus defining valid trivariate normal PDFs.

Two alternative dynamic EDs are evaluated for formamide. One is also a convoluted ED but without correlations in the nuclear vibrations, that is, only the block diagonal elements of the total MSDA matrix are included in the convolution ($\langle\rho(\boldsymbol{r})_{block}\rangle_T$). This approach closely resembles the formalism used to model Bragg diffraction data from which no covariance information can be retrieved. The other one is obtained as an average over a large ensemble of static EDs (sample size; $M = 5\cdot 10^5$) generated by sampling the nuclear configuration space (using the nuclear PDFs due to the B3LYP/6-311G** normal-modes) and mapping each member of this ensemble onto a corresponding single-point electronic wave function. The sample mean of the corresponding EDs $\left(\overline{\rho(\boldsymbol{r})} = M^{-1}\sum\rho_i(\boldsymbol{r},\boldsymbol{R}_i)\right)$ can be considered as the 'correct' thermal-average ED (within the time independent BO approach), since its evaluation does not rely on the convolution approximation; each member of the ED set is consistent with one and only one nuclear configuration [36].

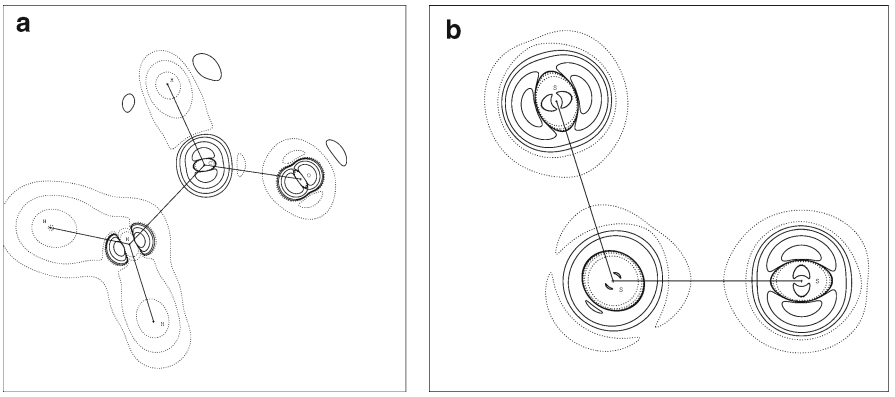

Fig. 1 Difference ED ($\langle\rho(\boldsymbol{r})\rangle_T - \rho(\boldsymbol{r})$) contur maps: (**a**, *left*) Formamide in the molecular plane, (**b**, *right*) octasulfur in the plane defined by three S-atoms. Contour levels are $\mp(0.01, 0.05, 0.25, 1.25)e/\text{Å}^3$, *solid/dotted lines* are positive/negative

One of the striking results of this simulation is that the static and the related dynamic EDs exhibit an overall fair agreement, except for the NH_2 group of the formamide molecule. Figure 1 displays difference ED contour maps ($\langle\rho(\boldsymbol{r})\rangle_T - \rho(\boldsymbol{r})$) in the molecular plane of formamide (1a) and in the plane defined by three consecutive S-atoms of the octasulfur molecule (1b). These maps well demonstrate the effect of nuclear vibrations; charge migrations from near-nuclear regions towards internuclear regions.

The BCP properties of the two EDs (Table 1) are very close in value. Even the largest differences, obtained for the positive eigenvalues of the Hessian at the BCP (λ_3), remain below 10 % for bonds formed between massive atoms. However, no BCP is found for any of the N–H bonds based on the dynamic EDs; neither for the convoluted ($\langle\rho(\boldsymbol{r})\rangle_T$, $\langle\rho(\boldsymbol{r})_{block}\rangle_T$) nor for the averaged ($\bar{\rho}$). These results are consistent with those found for the 'experimental' ED of trialanine [37] by the maximum entropy method which reconstructs the dynamic ED from diffraction data without having resource to any thermal smearing and static ED model.

On Fig. 2a the difference density ($\langle\rho(\boldsymbol{r})_{block}\rangle_T) - \langle\rho(\boldsymbol{r})\rangle_T$) in the plane of the formamide molecule reveals that the independent nuclear vibration model (block diagonal representation) is in a close agreement with that obtained by the correlated model using the full MSDA. The maximum error is only 0.015 e/Å^3, which occurs at the location of the Nitrogen nucleus. Figure 2b shows the difference in ($\overline{\rho(\boldsymbol{r})} - \langle\rho(\boldsymbol{r})\rangle_T$) where a quantitative comparison highlights that the maximum absolute error for formamide is only 1.45 e/Å^3 found at the nucleus of the oxygen atom.

Figure 3 compares the Laplacian of the static ($\nabla^2\rho$) and dynamic ($\nabla^2\langle\rho(\boldsymbol{r})\rangle_T$) EDs along the C=O (3a) and S–S (3b) bond paths. While a surprisingly good agreement is found in the near-BCP region for both bonds (distances C-BCP = 0.4153 Å, S-BCP=1.0297 Å), the residual functions ($\nabla^2\langle\rho(\boldsymbol{r})\rangle_T - \nabla^2\rho(\boldsymbol{r})$) exhibit pronounced differences in the vicinity of the valence-shell charge concentrations, especially for the polar C=O bond. These findings correlate well with the experimental irreproducibil-

Table 1 Topological Properties at BCPs of static and dynamic EDs of formamide and octasulfur (units are in e and Å)

Bond	Property	Static $\rho(\boldsymbol{r})$	Convolution $\langle\rho(\boldsymbol{r})\rangle_T$	Mean $\bar{\rho}(\boldsymbol{r})$
C–H	ρ	1.86	1.79	1.80
	$\nabla^2\rho$	−22.58	−22.90	−23.39
	λ_1	−18.00	−16.55	−16.87
	λ_2	−17.57	−16.29	−16.57
	λ_3	12.99	9.94	10.05
C–N	ρ	2.13	2.12	2.13
	$\nabla^2\rho$	−21.09	−20.07	−20.15
	λ_1	−16.38	−16.22	−16.37
	λ_2	−14.91	−14.83	−15.11
	λ_3	10.20	10.98	11.33
C–O	ρ	2.80	2.79	2.80
	$\nabla^2\rho$	−5.20	−2.90	−2.63
	λ_1	−25.97	−25.76	−25.98
	λ_2	−24.25	−24.18	−24.40
	λ_3	45.03	47.05	47.74
S–S	ρ	1.00	0.99	
	$\nabla^2\rho$	−2.69	−2.78	
	λ_1	−4.04	−3.98	
	λ_2	−4.00	−3.93	
	λ_3	5.35	5.14	

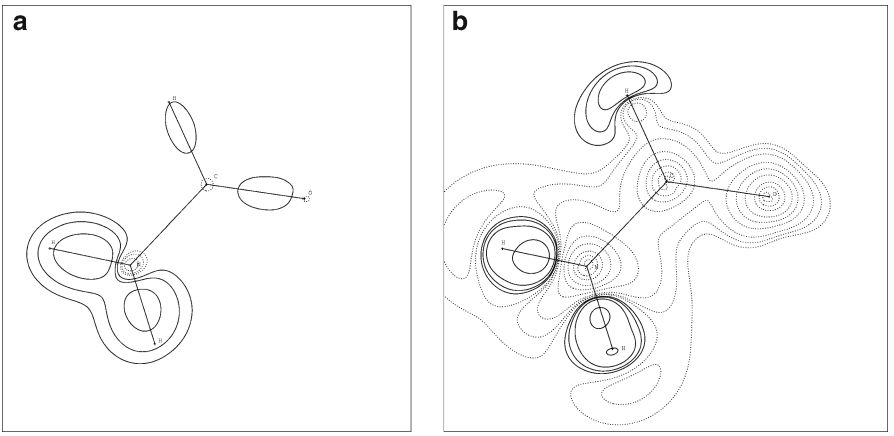

Fig. 2 Comparison of different dynamic EDs for Formamide: (**a**, *left*) the difference between the convoluted EDs calculated with the full and block-diagonal MSDA matrix ($\langle\rho(\boldsymbol{r})_{block}\rangle_T - \langle\rho(\boldsymbol{r})\rangle_T$), (**b**, *right*) the difference between the mean and the convoluted EDs ($\bar{\rho}(\boldsymbol{r}) - \langle\rho(\boldsymbol{r})\rangle_T$). Contour levels are at $\{\mp 2^n\}_{n=1,2,3}\,10^{-3}$, $\{\mp 2^n\}_{n=1,2,3}\,10^{-2}$, $\{\mp 2^n\}_{n=1,2,3}\,10^{-1}\,\mathrm{e}/\mathrm{Å}^3$, *solid/dotted lines* are positive/negative

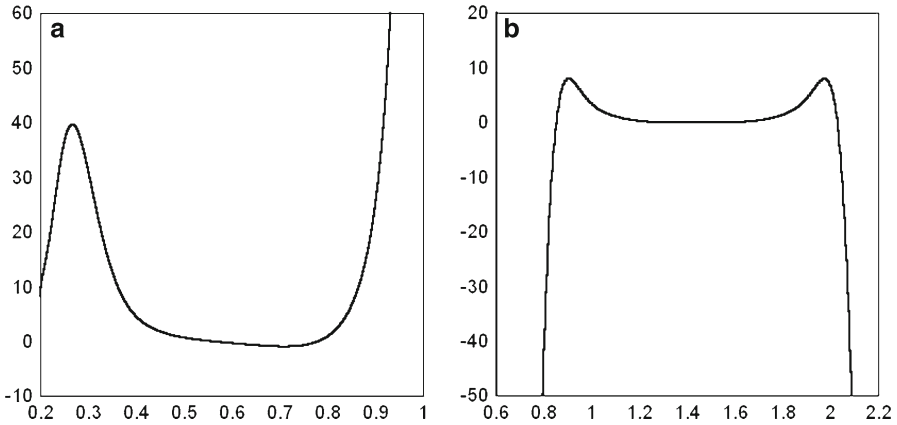

Fig. 3 The dynamic Laplacian with reference to that of the static $(\nabla^2\langle\rho(\boldsymbol{r})\rangle_T - \nabla^2\rho(\boldsymbol{r}))$ along (**a**, *left*) the C=O bond for the formamide molecule and (**b**, *right*) the S–S bond in the octasulfur molecule. Unit is $e/\text{Å}^5$

ity of the profiles of C=O bonds [1] which might suggest incomplete decoupling of thermal smearing effects and static density topology from X-ray structure factors [7].

5 Conclusion

A straightforward formalism is presented to calculate the dynamic molecular ED from that of the stationary ED within the harmonic convolution approximation and the LCAO-MO formalism utilizing Gaussian basis functions. In spite of its simplicity, the method turns out to provide a very accurate estimation of the thermally smeared ED ($\bar{\rho}$) obtained by a more rigorous and computationally much more demanding procedure that involves averaging over a large ensemble of single-point static EDs. This is well substantiated by the closeness of the BCP values obtained for the two dynamic EDs in Table 1. Even more surprisingly, the static and convoluted dynamic EDs are also found to exhibit a high degree of similarity in terms of BCP properties. However, for molecules containing hydrogen atoms, the two EDs do not necessarily reveal a topological equivalence. The convoluted ED for the formamide molecule, for example, exhibits no BCP for the N–H bonds because the hydrogen density peaks (the (3,−3) critical points of the static ED) are completely 'washed out' by thermal vibrations (became saddle points) even at such a low temperature as 23 K at which only the ground vibration states are populated. This result is of significance to the reliability of X-ray charge density based topological analyses of hydrogen bonds. The majority of these studies rely on higher-temperature diffraction data (typically around 100K) and the data interpretation utilizes either isotropic temperature factors for the H-atoms [38,39] or (preferably) ADPs from independent observations/calculations [40,41], making thus the experimental static ED for both covalent and non-covalent interactions involving H-atoms decisively model dependent. While this issue is quite widely recognized, the invisibility of the N–H bond path for the convoluted theoretical

ED, as shown in this study, indirectly implies that the results of topological analysis of experimental EDs of bonding involving H-atoms is not just simply supported, but entirely settled by the choice of the H-atom ADPs and mean positions. To be more precise, the 'experimental static' topology of H-bonding is a manifestation of parameters directly not observable by X-ray diffraction. To reach this conclusion one should just consider what it would take to solve the inverse problem, that is, to reconstruct fine topological details of the static ED for the N–H bonds from that of the convoluted dynamic ED for formamide.

It is to be emphasized that our analysis is restricted to internal (intra-molecular) vibrations of relatively high frequencies and thus low amplitudes. The inclusion of external modes (translation and rotation within the molecular mean field model [42]) or acoustic modes (within lattice dynamics [43]) is most likely to further demolish characteristic features of the static topology. A more general conclusion is that smearing the theoretical ED to compare it with the experimental ED deserves more attention than it has received during the most recent X-ray charge density era. After all, the molecular static ED is not a direct physical observable.

References

1. T.S. Koritsanszky, P. Coppens, Chemical applications of X-ray charge density analysis. Chem. Rev. **101**, 1583–1628 (2001)
2. C. Gatti, Chemical bonding in crystals: new directions. Z. f. Krist **220**, 399–487 (2005)
3. R.F.W. Bader, *Atoms in Molecules—a Quantum Theory* (Oxford University Press, New York, 1990)
4. R.F. Stewart, One-electron density functions and many-centered finite multipole expansions. Isr. J. Chem. **16**, 124–131 (1977)
5. N.K. Hansen, P. Coppens, Testing aspherical atom refinements on small molecule data sets. Acta Cryst. **A34**, 909–921 (1978)
6. F.L. Hirshfeld, Charge deformation and vibrational smearing. Isr. J. Chem. **16**, 168–174 (1977)
7. R. Flaig, T. Koritsanszky, D. Zobel, P. Luger, Topological analysis of experimental electron densities of amino acids: 1. D,L-aspartic acid at 20K. J. Am. Chem. Soc. **120**, 2227–2236 (1998)
8. E.D. Stevens, J. Rys, P. Coppens, Calculation of dynamic electron distributions from static molecular wavefunctions. Acta Cryst. **A33**, 333–338 (1977)
9. E.D. Stevens, J. Rys, P. Coppens, Quantitative comparison of theoretical calculations with experimental measurements. J. Am. Chem. Soc. **99**, 265–267 (1977)
10. P. Coppens, T.V. Willoughby, L.N. Csonka, Electron population analysis of accurate diffraction data. I. Formalism and restrictions. Acta Cryst. **A27**, 248–256 (1971)
11. S. Howard, J.P. Hulke, P.R. Mallinson, C.S. Frampton, Density matrix refinement for molecular crystals. Phys. Rev. **B49**(11), 7124–7136 (1994)
12. H. Schmider Jr, V.H. Smith, W. Weyrich, Reconstruction of the one particle density matrix from expectation values in position and momentum space. J. Chem. Phys. **96**(12), 8486–8994 (1992)
13. D. Jayatilaka, D.J. Grimwood, wavefunctions derived from experiment, I. Motivation and theory. Acta Cryst. **A57**, 76–86 (2001)
14. M. Born, K. Huang, *Dynamical Theory of Crystal Lattices* (Oxford University Press, Oxford, 1954)
15. M. Born, J.R. Oppenheimer, Zur Quantentheorie der Molekeln. Ann. Phys. **389**(20), 457–484 (1927)
16. C.A. Coulson, M.W. Thomas, The effect of molecular vibrations on apparent bond length. Acta Cryst. **B27**, 1354–1359 (1971)
17. A.F.J. Ruysink, A. Vos, Theoretical calculation of the time-averaged electron density distribution for vibrating ethylene molecules in a model crystal structure. Acta Cryst. **A30**, 497–502 (1974)
18. M. Messeschmidt, S. Scheins, P. Luger, Charge density of 9-0-strychnine from 100 to 15 K, a comparison of four data sets. Acta Cryst. **B61**, 115–121 (2005)
19. J. Oddershede, S. Larsen, Charge density study of naphthalene based on X-ray diffraction data at four different temperatures and theoretical calculations. J. Phys. Chem. **A108**, 1057–1063 (2004)

20. R. Destro, Presti L. Lo, R. Soave, A.E. Goeta, Multi-temperature electron density studies, in *Modern Charge Density Analysis*, ed. by C. Gatti, P. Macchi (Springer, Berlin, 2012)
21. M. Born, V.A. Fock, Beweis des Adiabatensatzes. Z. f. Phys. A **51**(3–4), 165–180 (1928)
22. Gaussian 09, Revision D.01, M.J. Frisch, G.W. Trucks, H.B. Schlegel, G.E. Scuseria, M.A. Robb, J.R. Cheeseman, G. Scalmani, V. Barone, B. Mennucci, G.A. Petersson, H. Nakatsuji, M. Caricato, X. Li, H.P. Hratchian, A.F. Izmaylov, J. Bloino, G. Zheng, J.L. Sonnenberg, M. Hada, M. Ehara, K. Toyota, R. Fukuda, J. Hasegawa, M. Ishida, T. Nakajima, Y. Honda, O. Kitao, H. Nakai, T. Vreven, J.A. Montgomery, Jr., J.E. Peralta, F. Ogliaro, M. Bearpark, J.J. Heyd, E. Brothers, K.N. Kudin, V.N. Staroverov, R. Kobayashi, J. Normand, K. Raghavachari, A. Rendell, J.C. Burant, S.S. Iyengar, J. Tomasi, M. Cossi, N. Rega, J.M. Millam, M. Klene, J.E. Knox, J.B. Cross, V. Bakken, C. Adamo, J. Jaramillo, R. Gomperts, R.E. Stratmann, O. Yazyev, A.J. Austin, R. Cammi, C. Pomelli, J.W. Ochterski, R.L. Martin, K. Morokuma, V.G. Zakrzewski, G.A. Voth, P. Salvador, J.J. Dannenberg, S. Dapprich, A.D. Daniels, Ö. Farkas, J.B. Foresman, J.V. Ortiz, J. Cioslowski, D.J. Fox, Gaussian Inc, Wallingford CT (2009)
23. A. Volkov, T. Koritsanszky, M. Chodkiewicz, H.F. King, On the basis-set dependence of local and integrated electron density properties: application of a new computer program for quantum-chemical density analysis. J. Comput. Chem. **30**, 1379–1391 (2009)
24. R.F. Stewart, D. Feil, A theoretical study of elastic X-ray scattering. Acta Cryst. **A36**, 503–509 (1980)
25. P.W. Higgs, Vibrational modificatios of the electron density in molecular crystals. II. Mean squares amplitudes of thermal motion. Acta Cryst. **8**, 99–104 (1955)
26. R.F. Stewart, Vibrational averaging of X-ray-scattering intensities. Isr. J. Chem. **16**, 137–143 (1997)
27. P. Debye, Interferenz von Röntgenstrahlen und Wärmebewegung. Ann. Phys. **348**, 49–92 (1913)
28. I. Waller, Zur Frage der Einwirkung der Wärmebewegung auf die Interferenz von Röntgenstrahlen. Z. Phys. **A17**, 398–408 (1923)
29. C. Scheringer, Temperature factors for internuclear density units. I. Theory in the harmonic approximation. Acta Cryst. **A33**, 426–429 (1977)
30. R.F. Stewart, Generalized X-ray scattering factors. J. Chem. Phys. **51**, 4569–4576 (1968)
31. K. Tanaka, X-ray analysis of wavefunctions by the least-squares method incorporating orthonormality. I. General formalism. Acta Cryst. **A44**, 1002–1008 (1988)
32. S.F. Boys, Electronic wave functions. I. A general method of calculation for the stationary states of any molecular system. Proc. R. Soc. Lond. Ser. **A200**, 542 (1950)
33. A.D. Becke, Density-functional exchange-energy approximation with correct asymptotic behavior. Phys. Rev. A **38**(6), 3098–3100 (1988)
34. C. Møller, M.S. Plesset, Note on an approximation treatment for many-electron systems. Phys. Rev. **46**, 618–622 (1934)
35. E.D. Stevens, J. Rys, P. Coppens, Quantitative comparison of theoretical calculations with the experimentally determined density distribution of formamide. J. Am. Chem. Soc. **100**, 2324–2328 (1978)
36. J.R. Michael, T. Koritsanszky, Computational study of uncertainties of local topological properties of the molecular electron density (in preparation)
37. A. Hofmann, J. Netzel, S. van Smaalen, Accurate charge density of trialanine: a comparison of multipole formalism and the maximum entropy method. Acta Cryst. **B63**, 285–295 (2007)
38. E. Espiosa, E. Mollins, C. Lecomte, Hydrogen bond strengths revealed by topological analyses of experimentally observed electron densities. Chem. Phys. Lett. **285**, 170–173 (1988)
39. P. Munshi, T.N. Guru Row, Intra-and intermolecular interaction in small bioactive molecules: cooperative features from experimental and theoretical charge density analysis. Acta Cryst. **B62**, 612–626 (2006)
40. A.O. Madsen, H.O. Sorensen, C. Flensburg, R.F. Stewart, S. Larsen, Modeling of the nuclear parameters of H atoms in X-ray charge density studies. Acta Cryst. **A60**, 550–561 (2004)
41. P. Roversi, R. Destro, Approximate anisotropic displacement parameters for H atoms in molecular crystals. Chem. Phys. Lett. **386**, 472–478 (2004)
42. H.B. Bürgi, S.C. Capelli, Dynamics of molecules in crystals from multi-temperature anisotropic parameters. I. Theory. Acta Cryst. **A56**, 403–412 (2000)
43. A.O. Madsen, B. Civalleri, M. Ferrabone, F. Pascale, A. Erba, Anisotropic displacement parameters for molecular crystals from periodic Hartree–Fock and density functional calculations. Acta Cryst. **A69**, 309–321 (2013)